Voltammetric studies of the interaction of the lithium cation with reduced forms of the Dawson [S 2Mo 18O 62] 4− polyoxometalate anion

ARTICLE *in* JOURNAL OF ELECTROANALYTICAL CHEMISTRY · DECEMBER 2000

Impact Factor: 2.87 · DOI: 10.1016/S0022-0728(00)00275-8

ELSEVIER

www.elsevier.nl/locate/jelechem

Journal of Electroanalytical Chemistry 494 (2000) 96–104

Journal of Electroanalytical Chemistry

Voltammetric studies of the interaction of the lithium cation with reduced forms of the Dawson $[S_2Mo_{18}O_{62}]^{4-}$ polyoxometalate anion

Alan M. Bond [a,*], Truc Vu [a], Anthony G. Wedd [b]

[a] *Department of Chemistry, Monash University, Clayton, Vic. 3168, Australia*
[b] *School of Chemistry, University of Melbourne, Parkville, Vic. 3052, Australia*

Received 18 October 1999; received in revised form 18 May 2000; accepted 19 May 2000

Abstract

Multiple electron transfer steps observed in the reduction of $[S_2Mo_{18}O_{62}]^{4-}$, when $LiClO_4$ is used as electrolyte, are accounted for by assuming that Li^+ acts as a moderately strong Lewis acid. For example, in the 95:5 $CH_3CN + H_2O$ solvent mixture (0.1 M NBu_4ClO_4), the voltammetric behavior obtained on addition of Li^+ can be simulated according a reaction scheme involving an extensive series of reversible potentials and equilibrium constants. Precipitation of highly reduced polyoxometalate salts occurring at the electrode surface complicates the voltammetry at very negative potentials when 0.1 M $LiClO_4$ is used as the electrolyte.

Keywords: Lithium cation; Dawson polyoxometalate anion; Voltammetry

1. Introduction

Polyoxometalates are being studied extensively for their interesting photochemical, catalytic and redox properties which find application in commercial processes and technologies [1–15].

Voltammetric studies on polyoxometalate complexes have commonly revealed the presence of an extensive series of reduction processes [3,15]. Many early studies on Keggin and Dawson polyoxometalates were undertaken in aqueous media in the presence of acid or metal ion salts as electrolyte. In neutral aqueous media and for Keggin anions, the multiple electron steps detected in the presence of acid split into single electron steps. In the case of initial studies on Dawson complexes, even numbers of two, four, six or more electrons were always transferred in each step [16], so that the existence of the odd one-electron reduced states was uncertain [17–20]. However, more recently, use of aprotic solvents with tetraalkylammonium salts as electrolytes has also revealed the presence of the odd one-electron configuration with the Dawson anions [21–24].

For the reduction of the $[S_2Mo_{18}O_{62}]^{4-}$ Dawson anion in acidic (95:5) $CH_3CN + H_2O$ media, the presence of acid–base equilibria coupled with electron transfer quantitatively accounts for the transformation of a series of reversible one-electron reduction processes to a more extensive series of chemically reversible processes [25]. The latter processes involve the overall transfer of an even number of electrons. Thus, in the absence of acid, the initial four one-electron reduction steps occur as in Eq. (1).

$$[S_2Mo_{18}O_{62}]^{4-} + e^- \leftrightharpoons [S_2Mo_{18}O_{62}]^{5-} + e^- \leftrightharpoons [S_2Mo_{18}O_{62}]^{6-} + e^- \leftrightharpoons [S_2Mo_{18}O_{62}]^{7-} + e^- \leftrightharpoons [S_2Mo_{18}O_{62}]^{8-} \quad (1)$$

In contrast, in the presence of aqueous perchloric acid, the four electrons are transferred in two steps Eq. (2):

$$[S_2Mo_{18}O_{62}]^{4-} + 2H^+ + 2e^- \leftrightharpoons [H_2S_2Mo_{18}O_{62}]^{4-} + 2H^+ + 2e^- \leftrightharpoons [H_4S_2Mo_{18}O_{62}]^{4-} \quad (2)$$

* Corresponding author. Tel.: +61-3-99051338; fax: +61-3-99059129.
E-mail address: alan.bond@sci.monash.edu.au (A.M. Bond).

0022-0728/00/$ - see front matter
PII: S0022-0728(00)00275-8

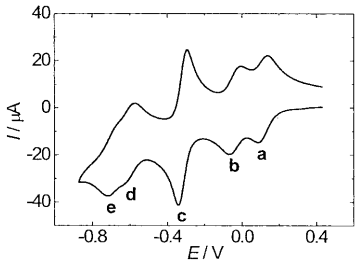

Fig. 1. Cyclic voltammogram obtained at a glassy carbon macrodisk electrode ($d = 2.8$ mm) using a scan rate of 0.1 V s^{-1} for the reduction of 1 mM $[NHex_4]_4[S_2Mo_{18}O_{62}]$ in $CH_3CN + 0.1$ M $LiClO_4$.

Coupling of electron transfer and acid–base equilibria also accounted for the transformation of a series of one-electron processes into apparently multiple-electron processes in the reduction of $[P_2W_{18}O_{62}]^{6-}$ and $[H_2W_{12}O_{40}]^{6-}$ [26].

In view of the common detection of multi-electron even numbered electron process when metal salts have been used as an electrolyte, we have examined the particular case of $LiClO_4$ as an electrolyte to ascertain whether the Li^+ cation effectively acts as a Lewis acid and hence produces voltammetric behavior analogous to that observed in the presence of H^+. We report a quantitative study of the voltammetric reduction of $[S_2Mo_{18}O_{62}]^{4-}$ in the presence of Li^+ to achieve an enhanced understanding of the role of the lithium cation in polyoxometalate redox chemistry.

2. Experimental

2.1. Reagents and compounds

Electrometric grade NBu_4ClO_4 (GFS) and reagent grade $LiClO_4$ (BDH) were used as the electrolytes. The solvent, CH_3CN was HPLC grade, 99.9% (Mallinckrodt). $[NHex_4]_4[S_2Mo_{18}O_{62}]$ was synthesized as in Ref. [23].

2.2. Electrochemistry

All voltammograms were acquired at (22 ± 1)°C using a Cypress Systems model CS-1090 computer-controlled electroanalytical system in the staircase mode.

A standard three electrode chemical cell arrangement was employed with a glassy carbon disk ($d = 3.0$ mm), or a glassy carbon rotating disk [diameter (d) = 2.8 mm] electrode as the working electrode, a platinum wire as the counter electrode and a $Ag \mid Ag^+$ (0.01 M $AgNO_3$) reference electrode separated from the test solution by a porous frit. Rotating disk electrode experiments were undertaken with a variable speed rotator (Metrohm 628-10). All electrode potentials are quoted relative to the ferrocene/ferricenium redox couple (Fc/Fc^+). Prior to each voltammetric experiments, solutions were degassed with nitrogen that had been pre-saturated with the appropriate solvents.

Digital simulations of cyclic voltammograms were performed by using the simulation package DIGISIM V 2.1 (Bioanalytical System, West Lafayette, IN) and were run on 150 MHz Pentium PC [26,27].

3. Results and discussion

3.1. Electrochemistry in CH_3CN

3.1.1. Cyclic voltammetry at a macrodisk glassy carbon electrode

A cyclic voltammogram obtained at a scan rate (v) of 0.1 V s^{-1} for the reduction of 1 mM $[S_2Mo_{18}O_{62}]^{4-}$ in CH_3CN (0.1 M $LiClO_4$) at a glassy carbon macrodisk electrode over the potential range 0.42 to -0.88 V versus Fc/Fc^+ exhibits five chemically reversible processes (**a**, **b**, **c**, **d** and **e** in Fig. 1). The $E_{1/2}$-values calculated as $(E_p^{red} + E_p^{ox})/2$ ($E_{1/2}$ = half-wave potential, E_p^{red} = reduction peak potential, E_p^{ox} = oxidation peak potential) are given in Table 1. Processes **a**, **b** and **c** are well separated, while processes **d** and **e** are partially

Table 1
Cyclic voltammetric parameters for 1 mM $[NHex_4]_4[S_2Mo_{18}O_{62}]$ in $CH_3CN + 0.1$ M $LiClO_4$

Process [a]	E_p^{red}/V [b]	E_p^{ox}/V [b]	$E_{1/2}$/V [b]	ΔE_{p-p}/V	I_p^{red}/μA	I_p^{red}/I_p^{ox}
a	0.09	0.15	0.12	0.06	−18.5	0.97
b	−0.07	−0.01	−0.04	0.06	−15.4	0.95
c	−0.34	−0.30	−0.32	0.04	−38.5	1.00
d	−0.62	−0.57	−0.60	0.05 [c]	[d]	[d]
e	−0.72	−0.68	−0.70	0.04 [c]	[d]	[d]

[a] Glassy carbon macrodisk electrode ($d = 2.8$ mm); v, 0.1 V s^{-1}.
[b] V versus Fc/Fc^+.
[c] ± 10 mV due to overlap of process **d** and **e**.
[d] Peak current values not cited because of overlap of process **d** and **e**.

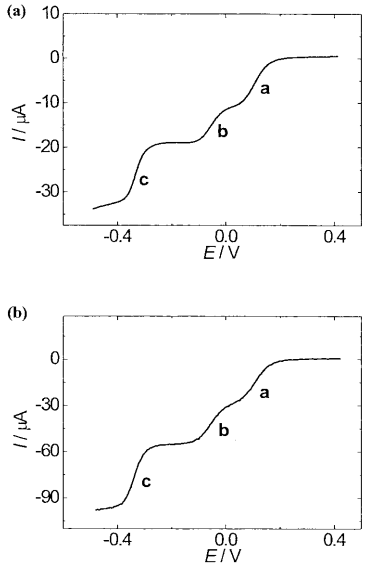

Fig. 2. (a) Microdisk and (b) rotating disk voltammogram for the reduction of 1 mM $[NHex_4]_4[S_2Mo_{18}O_{62}]$ in $CH_3CN + 0.1$ M $LiClO_4$. (a) platinum disk ($d = 75.0$ μm); v, 0.006 V s^{-1} and (b) glassy carbon macrodisk ($d = 2.8$ mm); $v = 0.01$ V s^{-1}; $\omega = 500$ rpm.

resolved. Additional processes observed at more negative potentials are complex and are not discussed further in this paper. Under the same voltammetric conditions but with 0.1 M NBu_4ClO_4 as electrolyte, three electrochemically reversible one-electron processes (**I**, **II** and **III**) were observed with $E_{1/2}$-values of 0.12, -0.12 and -0.78 V [24]. The influence of the electrolyte cation is obviously important.

The $E_{1/2}$-values of one-electron processes **a** and **I** are similar. However, that of process **b** (-0.04 V) is significantly more positive than that of process **II** (-0.12 V), although **b** retains characteristics that are close to those expected for a reversible one-electron reduction process (Table 1). In contrast, process **c** in 0.1 M $LiClO_4$ is distinctly different from the third process **III** in 0.1 M NBu_4ClO_4. Process **c** exhibits a peak current about twice that of processes **a** and **b**. This feature together, with a ΔE_p-value of 0.04 V ($\Delta E_p = E_p^{ox} - E_p^{red}$), suggests the presence of an overall multi-electron but still chemically reversible process, rather than a reversible one-electron event. Processes **d** and **e** are not well resolved, leading to uncertainty in estimated parameters (Table 1). However, a $\Delta E_p < 60$ mV suggests that these also are multi-electron processes (see later). Cyclic voltammograms obtained at scan rates over the range of 0.02–1 V s^{-1} confirm the chemical reversibility of all five processes **a**–**e**.

3.1.2. Near steady-state voltammetry using a microdisk electrode

The near steady-state voltammogram for reduction of 1 mM $[S_2Mo_{18}O_{62}]^{4-}$ in $CH_3CN + 0.1$ M $LiClO_4$ obtained at a platinum microdisk electrode (diameter, $d = 75.0$ μm) for the initial three reduction processes (**a**–**c**) is shown in Fig. 2(a). Processes **d** and **e** detected under conditions of cyclic voltammetry are not readily observable, suggesting that surface reactions giving rise to electrode blockage occur under these conditions of slow scan rate and high current density. The $E_{1/2}$ and limiting current values (I_L) of **a**–**c** as a function of microdisk size and electrode material are listed in Table 2.

$E_{1/2}$-values obtained are similar to those found under the conditions of cyclic voltammetry described above. However, the ratios of I_L values for **a**, **b** and **c** are a function of microdisk electrode size. At the 250 μm diameter platinum electrode, the ratio (1:0.8:1.7) is close to the values expected (1:1:2) if **c** is a two-electron reduction and processes **a** and **b** are one-electron steps. At the smaller 75 μm diameter platinum electrode, the ratio is (1:0.8:1.3). This presence of surface blockage which was suggested to be a reason for the absence of processes **d** and **e**, also probably accounts for the smaller than expected currents for steps **b** and **c** at the 75 μm diameter platinum microdisk electrode. However, each of processes **a**, **b** and **c** still could be detected at an 11 μm diameter glassy carbon microdisk electrode, so that both the nature of the electrode material and electrode size are important variables in the observed voltammetry.

The slopes of log-plots [E versus $\log(I_L - I)/I$] (I = current at potential E) for processes **a** and **b** are 0.056 and 0.052 V, respectively, at the 75 μm diameter platinum electrode (Table 2) and hence are close to the value expected for a reversible one-electron process

Table 2
Parameters for near steady state voltammetry of 1 mM $[NHex_4]_4[S_2Mo_{18}O_{62}]$ in $CH_3CN + 0.1$ M $LiClO_4$

Electrode d/μm	GC (11)		Pt (75)			Pt (250)	
Scan rate/V s^{-1}	0.01		0.006			0.002	
Process	$E_{1/2}$/V	I_L/nA	$E_{1/2}$/V	I_L/nA	Slope/V [a]	$E_{1/2}$/V	I_L/nA
a	0.12	−1.5	0.12	−10.8	0.056	0.12	−42.6
b	−0.06	−1.3	−0.06	−8.2	0.052	−0.06	−35.5
c	−0.30	−0.6	−0.32	−13.8	0.042	−0.33	−72.7

[a] Obtained from a plot of E versus $\log[(I_L - I)/I]$.

Table 3
Parameters for rotating disk voltammetry [a] of 1 mM $[NHex_4]_4[S_2Mo_{18}O_{62}]$ in $CH_3CN + 0.1$ M $LiClO_4$

Rotation	Process **a**			Process **b**			Process **c**		
Speed/rpm	$E_{1/2}$/V	I_L/μA	Slope/V [b]	$E_{1/2}$/V	I_L/μA	Slope/V [a]	$E_{1/2}$/V	I_L/μA	Slope/V [a]
500	0.12	−27.8	0.059	−0.06	−25.1	0.059	−0.33	−39.2	0.042
1000	0.12	−38.6		−0.06	−35.0		−0.33	−33.0	
1500	0.12	−49.1		−0.05	−42.5		−0.34	−21.4	
2000	0.12	−55.5		−0.04	−45.2		−0.30	−11.9	

[a] Glassy carbon macrodisk electrode ($d = 2.8$ mm); $v = 0.01$ V s^{-1}.
[b] Obtained from a plot of E versus $\log[(I_L - I)/I]$.

$(0.058/n)$. In contrast, the log-plot slope of process **c** was 0.042 V, which is consistent with two unresolved one-electron processes.

3.1.3. Voltammetry using a rotating disk electrode

Rotating macrodisk electrode experiments were examined in an attempt to minimize problems attributed to electrode blockage at microdisk electrodes. A steady-state voltammogram at glassy carbon is shown in Fig. 2(b) and parameters for processes **a**–**c** are given in Table 3. The $E_{1/2}$-values obtained at a rotation speed of 500 rpm are similar to those found using a microdisk electrode. The slopes of the E versus $\log[(I_L - I)/I]$ plots for **a** and **b** are close to the value of 0.058 V expected for a reversible one-electron transfer. In contrast, the slope for process **c** is 0.042 V, again suggesting that transfer of more than one-electron is involved. The limiting currents of processes **a** and **b** increase linearly as a function of the square root of rotation rate (ω) as predicted by the Levich equation for a mass transport limited process (Table 3, Fig. 3). That of process **c** actually decreases as the rotation rate is increased (Fig. 3). This decrease becomes even more pronounced at slower scan rates. When the rotation speed is greater than 1000 rpm and the scan rate of the potential is 0.005 V s^{-1}, almost complete blockage of the electrode surface occurs after the potential of process **b** has been reached (Fig. 4). In addition, processes **d** and **e** again are not detected using this technique, presumably because of surface blockage. Apparently, at the high current densities obtained with fast rotation of an electrode or use of a very small electrode, the solubility of a lithium salt of two-electron reduced $[S_2Mo_{18}O_{62}]^{6-}$ is exceeded and precipitation of solid occurs at a kinetically controlled rate onto the electrode surface, causing electrode blockage.

In summary, in the presence of $LiClO_4$, the first two reduction processes **a** and **b** appear to involve chemically reversible one-electron steps (Eqs. (3) and (4)). Process **c** on the basis of ΔE_p-values from cyclic voltammetry and slope of log-plot analyses under steady-state conditions is believed to involve a chemically reversible overall two-electron transfer as described in Eq. (5).

$$[S_2Mo_{18}O_{62}]^{4-} + e^- \rightleftharpoons [S_2Mo_{18}O_{62}]^{5-} \quad (3)$$

$$[S_2Mo_{18}O_{62}]^{5-} + e^- \rightleftharpoons [S_2Mo_{18}O_{62}]^{6-} \quad (4)$$

$$[S_2Mo_{18}O_{62}]^{6-} + 2e^- \rightleftharpoons [S_2Mo_{18}O_{62}]^{8-} \quad (5)$$

Processes **d** and **e** are more difficult to characterize but are almost certainly multi-electron step processes and they can be assigned tentatively as chemically reversible overall two-electron processes (Eqs. (6) and (7)).

$$[S_2Mo_{18}O_{62}]^{8-} + 2e^- \rightleftharpoons [S_2Mo_{18}O_{62}]^{10-} \quad (6)$$

$$[S_2Mo_{18}O_{62}]^{10-} + 2e^- \rightleftharpoons [S_2Mo_{18}O_{62}]^{12-} \quad (7)$$

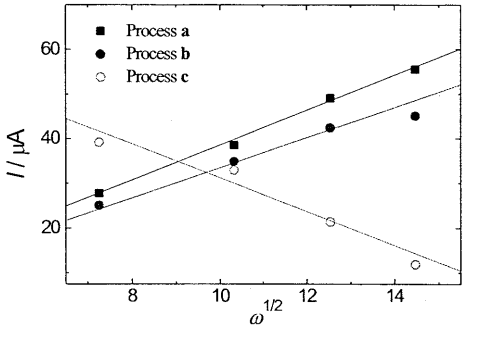

Fig. 3. Plot of I_L versus $\omega^{1/2}$ obtained at a glassy carbon rotating disk electrode ($d = 2.8$ mm) for the reduction of 1 mM $[NHex_4]_4[S_2Mo_{18}O_{62}]$ in $CH_3CN + 0.1$ M $LiClO_4$ using a scan rate of 0.01 V s^{-1}.

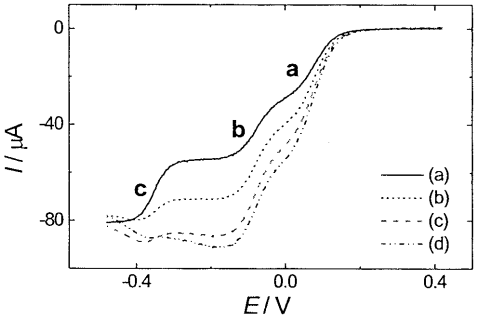

Fig. 4. Steady-state hydrodynamic voltammograms obtained at a glassy carbon rotating disk electrode ($d = 2.8$ mm) using a scan rate of 0.005 V s^{-1} for the reduction of 1 mM $[NHex_4]_4[S_2Mo_{18}O_{62}]$ in $CH_3CN + 0.1$ M, $LiClO_4$ at rotation speeds of: (a) 500; (b) 1000; (c) 1500; and (d) 2000 rpm.

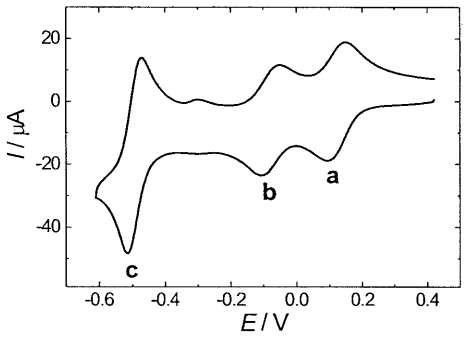

Fig. 5. Cyclic voltammogram obtained at a glassy carbon macrodisk electrode ($d = 3.0$ mm), scan rate of 0.05 V s^{-1} for the reduction of 1 mM $[NHex_4]_4[S_2Mo_{18}O_{62}]$ in 95:5 $CH_3CN + H_2O$ (v/v) + 0.1 M $LiClO_4$.

For simplicity terms associated with Li^+ have been omitted in all equations at this stage, but clearly the role of this cation in the voltammetry must be important.

3.2. Electrochemistry in 95:5 $CH_3CN + H_2O$ (v/v)

3.2.1. Cyclic voltammetry

Previous studies aimed at establishing the role of the H^+ ion used perchloric acid addition in a 95:5 $CH_3CN + H_2O$ (v/v) mixed solvent medium [25]. The present work employed $LiClO_4$ in the same medium for an optimal comparison of the behavior of the two cations.

*3.2.1.1. Processes **a**–**c**.* A cyclic voltammogram of 1 mM $[S_2Mo_{18}O_{62}]^{4-}$ in 95:5 $CH_3CN + H_2O$ (v/v) + 0.1 M $LiClO_4$ at a glassy carbon macrodisk electrode ($d =$ 3.0 mm) detects processes **a**–**c** (Fig. 5) (a small surface based process is also detected between process **b** and **c**). Parameters are listed in Table 4. The $E_{1/2}$-value of process **a** is similar to that found in CH_3CN, whilst those of processes **b** and **c** occur at more negative potentials (compare data in Tables 2 and 4). In 95:5 $CH_3CN + H_2O$ (v/v), there would be a competitive reaction between reduced forms of $[S_2Mo_{18}O_{62}]^{4-}$ and $Li(CH_3CN)_x^+$ and $Li(OH_2)_6^+$. Hence, the expected stronger association of Li^+ with H_2O than CH_3CN [28,29] may explain why the $E_{1/2}$-values of process **b** and **c** are more negative when 5% water is present than those found in dry CH_3CN. That is, apparently interaction of Li^+ favors the more highly charged reduced forms and this causes a shift of the reduction processes to positive potentials. However, medium effects can be significant in determining the values of reversible potentials so that the contribution of the water itself cannot be neglected [15].

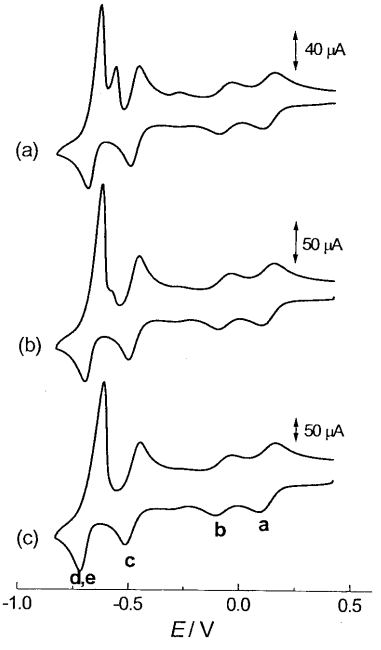

Fig. 6. Cyclic voltammograms at a glassy carbon macrodisk electrode ($d = 3.0$ mm) for the reduction of 1 mM $[NHex_4]_4[S_2Mo_{18}O_{62}]$ in 95:5 $CH_3CN + H_2O$ (v/v) + 0.1 M $LiClO_4$ using scan rates of: (a) 0.05; (b) 0.20; and (c) 1.0 V s^{-1}.

*3.2.1.2. Processes **d** and **e**.* When the potential is switched at -0.85 V, a fourth reduction process (**d**, **e**) in 95:5 $CH_3CN + H_2O$ is observed (Fig. 6), possibly as the unresolved four-electron analogue of the two partially resolved two-electron processes **d** and **e** detected

Table 4
Cyclic voltammetric parameters for 1 mM $[NHex_4]_4[S_2Mo_{18}O_{62}]$ in 95:5 $CH_3CN + H_2O$ (v/v) + 0.1 M, $LiClO_4$

Scan rates	0.05 V s^{-1}			1.0 V s^{-1}						
Process [a]	E_p^{red}/V	E_p^{ox}/V	$E_{1/2}$/V	I_p^{red}/μA	I_p^{ox}/μA	E_p^{red}/V	E_p^{ox}/V	$E_{1/2}$/V	I_p^{red}/μA	I_p^{ox}/μA
a	0.09	0.15	0.12	−10.0	9.6	0.09	0.15	0.12	−38.2	37.5
b	−0.11	−0.05	−0.08	−8.9	9.2	−0.11	−0.04	−0.08	−35.1	35.9
c	−0.51	−0.47	−0.49	−21.0	20.4	−0.46	−0.52	−0.49	−76.2	77.0
d, **e**	−0.70	−0.64 [b]		−22.8	59.5	−0.62	−0.73	−0.68	−98.5	260.0
		−0.57 [b]			17.2 [b]					

[a] Glassy carbon macrodisk electrode ($d = 2.8$ mm); $v = 0.01$ V s^{-1}.
[b] Process **d** and **e** become split on reverse or oxidative scan direction at slow scan rates.

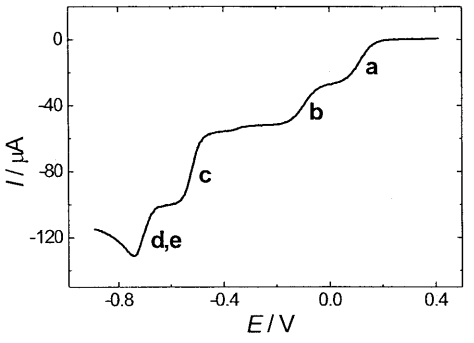

Fig. 7. Steady-state hydrodynamic voltammogram for the reduction of 1 mM $[NHex_4]_4[S_2Mo_{18}O_{62}]$ in 95:5 $CH_3CN + H_2O$ (v/v) + 0.1 M$LiClO_4$ at a glassy carbon rotating disk electrode (d, = 2.8 mm) using a scan rate of 0.10 V s^{-1} and rotation speed of 500 rpm.

in pure acetonitrile. At a scan rate of 0.2 V s^{-1}, I_p^{red} for process **d** and **e** is similar to that of process **c**, whilst at a scan rate of 1 V s^{-1} the peak height is larger. The stripping peaks now observed on the reverse scan imply that in the presence of water, that reduction leads to formation of an electroactive film of adsorbed or precipitated material on the electrode surface, which is rapidly removed by oxidation. Cyclic voltammetric data for process **d** and **e** are summarized in Table 4.

3.2.2. Steady-state voltammetry at a rotated disk electrode

Steady-state voltammograms of 1 mM $[S_2Mo_{18}O_{62}]^{4-}$ in 95:5 $CH_3CN + H_2O$ (v/v) + 0.1 M $LiClO_4$ at a glassy carbon rotating disk electrode, also show four major reduction processes over the potential range of interest and a minor process between process **b** and **c** (Fig. 7). Significantly, the current decays rapidly after the potential where process **d** and **e** occurs has been reached, as could be expected if precipitation of an insoluble product occurs and blocks the electrode surface. The $E_{1/2}$ and I_L values for each of the reduction processes at different rotation speeds are contained in Table 5. The $E_{1/2}$-values of processes **a** and **b** are similar to those obtained under conditions of cyclic voltammetry, while that for process **c** occurs at a slightly more negative potential. Linear plots of E versus $\log[(I_L - I)/I]$ are obtained for each of the first three reduction processes. The slopes for reduction processes **a** and **b** are each close to the expected value of 0.058 V for a one-electron transfer step. In contrast, the slope of reduction process **c** is 0.033 V, which is consistent with process **c** involving an overall two-electron charge transfer step.

3.3. Impact of the stepwise addition of $LiClO_4$

The role of the Li^+ cation is clearly revealed when small concentrations are added in a stepwise manner to a solution initially containing 0.1 M NBu_4ClO_4 as the electrolyte.

3.3.1. Differential pulse voltammetry

Differential pulse voltammograms in 95:5 $CH_3CN + H_2O$ (v/v) + 0.1 M NBu_4ClO_4 at a glassy carbon macrodisk electrode are shown in Fig. 8 as a function of $LiClO_4$ concentration. Upon stepwise addition of $LiClO_4$ over the concentration range of 0–0.3 mM, processes **I** and **II** (equivalent under the conditions to those previously labeled as **a** and **b**) remain unchanged, while processes **III** and **IV** merge and shift to a more positive potential to give the process now labeled **c** or (**III**, **IV**). This experiment confirms that process **c** is indeed an overall two-electron charge transfer process. Processes **d** and **e** are also observed after addition of Li^+. In the presence of 3.0 mM $LiClO_4$ the peak height of both processes **c**, **d** and **e** are considerably greater than **a** or **b**, but processes **d** and **e** are relatively broad. In the presence of 10 mM $LiClO_4$, process **I** (or **a**) remains unchanged, while processes **b**, **c**, **d** and **e** shift towards more positive potentials and the peak current for process **d** and **e** become significantly larger than that of **c**. Additionally, processes **d** and **e** are now very sharp and has the characteristic of an overall unresolved four-electron process as previously postulated.

3.3.2. Digital simulation

The results observed in the voltammetry of $[S_2Mo_{18}O_{62}]^{4-}$ upon stepwise addition of Li^+ are analogous to those observed upon addition of $HClO_4$

Table 5
Parameters for rotating disk voltammetry [a] of 1 mM $[NHex_4]_4[S_2Mo_{18}O_{62}]$ in 95:5 $CH_3CN + H_2O$ (v/v) + 0.1 M $LiClO_4$

Rotation	Process **a**		Process **b**		Process **c**		Process **d**, **e**	
Speed/rpm	$E_{1/2}$/V	I_L/μA	$E_{1/2}$/V	I_L/μA	$E_{1/2}$/V	I_L/μA	$E_{1/2}$/V	I_L/μA
500	0.12	−27.3	−0.08	−25.0	−0.51	−45.2	−0.69	−30.0
1000	0.12	−39.3	−0.08	−34.7	−0.51	−59.2	−0.69	−26.2
1500	0.12	−53.5	−0.09	−36.8	−0.51	−77.8	−0.71	−36.4
2000	0.12	−60.5	−0.09	−44.4	−0.51	−88.3	−0.71	−33.9
2500	0.12	−66.9	−0.10	−49.7	−0.52	−94.3	−0.71	−32.5
3000	0.12	−71.0	−0.10	−57.0	−0.52	−108.1	−0.71	−22.3

[a] Glassy carbon macrodisk electrode (d = 2.8 mm); v = 0.01 V s^{-1}.

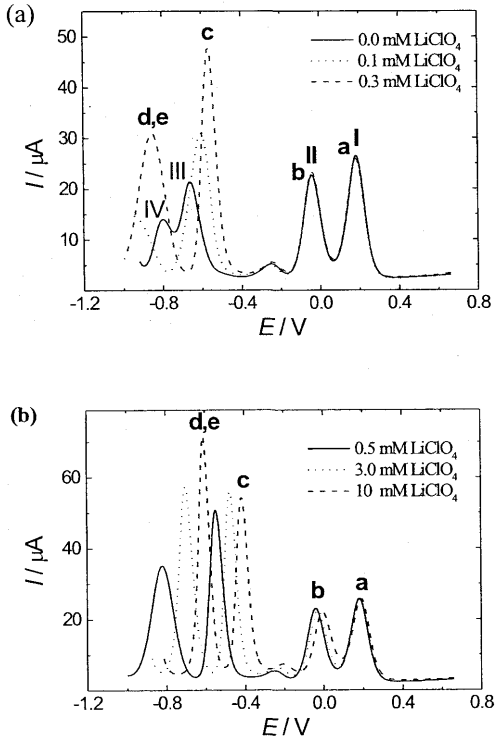

Fig. 8. Differential pulse voltammograms obtain as a function of added $LiClO_4$ concentration for reduction of 1 mM $[NHex_4]_4[S_2Mo_{18}O_{62}]$ in 95:5 $CH_3CN + H_2O$ (v/v) + 0.1 M NBu_4ClO_4 at a glassy carbon macrodisk electrode ($d = 3.0$ mm) with a pulse height of 0.05 V.

[25], except that Li^+ appears to act as a weaker acid than H^+. Fig. 9 provides a comparison of simulated and experimental voltammograms for the first three reduction processes. Scheme 1 used for the purpose of the simulation assumes that the primary charge transfer steps in the absence of Li^+ are reversible one-electron processes and that Li^+ equilibrium reactions accompany the generation of two-, three- and four-electron reduced species. Scheme 1 also evolved from the following additional considerations:

1. The oxidized form, $[S_2Mo_{18}O_{62}]^{4-}$, and the one-electron reduced species, $[S_2Mo_{18}O_{62}]^{5-}$, are assumed not to interact with Li^+, because $E_{1/2}$ for process **a** (Li^+ present) and **I** (Li^+ absent) are the same.
2. The diffusion coefficient [25] of $[S_2Mo_{18}O_{62}]^{4-}$ and all other polyoxometalate species were assumed to be 6.4×10^{-6} cm^2 s^{-1}. The diffusion coefficient for Li^+ was assumed to be 1.4×10^{-5} cm^2 s^{-1} in 95:5 $CH_3CN + H_2O$ (v/v) and hence significantly larger than for $[S_2Mo_{18}O_{62}]^{4-}$. The larger value for Li^+ was required for fitting of experimental and simulated voltammograms and is qualitatively in agreement with expectations based on other studies [26].
3. The four reversible $E_{1/2}$ values for the $[S_2Mo_{18}O_{62}]^{4-/5-}$, $[S_2Mo_{18}O_{62}]^{5-/6-}$, $[S_2Mo_{18}O_{62}]^{6-/7-}$ and $[S_2Mo_{18}O_{62}]^{7-/8-}$ processes (E_1–E_4) were estimated voltammetrically from data obtained in the absence of $LiClO_4$.

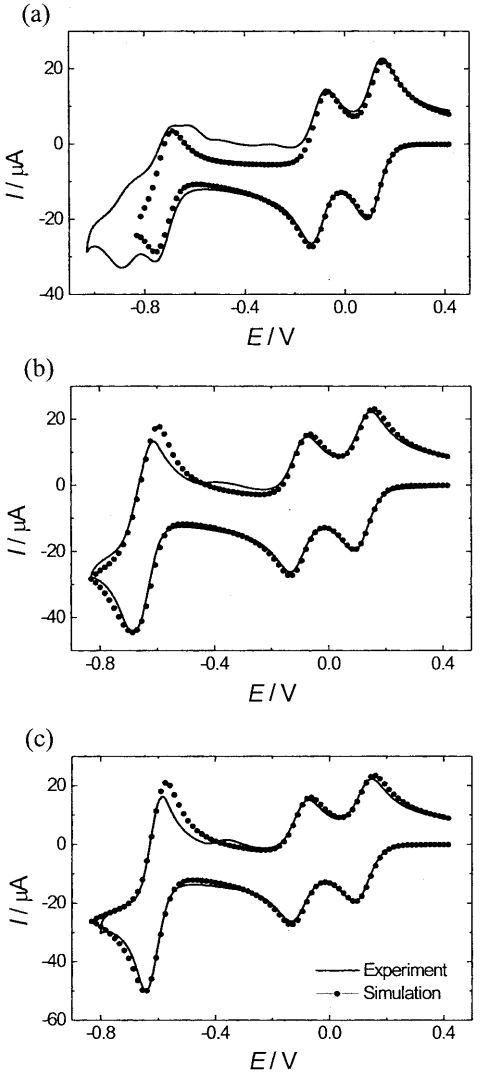

Fig. 9. Comparison of experimental and simulated (according to Scheme 1) cyclic voltammograms obtained in the presence of: (a) 0; (b) 0.2; and (c) 0.5 mM $LiClO_4$. Reversible potentials and equilibrium constant used for the simulation are contained in Table 6. Other experimental parameters are as for Fig. 5.

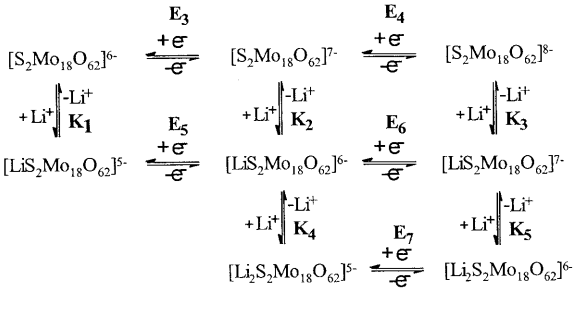

Scheme 1. Value of reversible potentials E_3–E_7 and equilibrium constant K_1–K_5 are contained in Table 6.

Table 6
Parameters used to simulate cyclic voltammograms [a,b]

Charge transfer reactions [c]	$E_{1/2}$/V
$[S_2Mo_{18}O_{62}]^{4-} + e^- \leftrightharpoons [S_2Mo_{18}O_{62}]^{5-}$	0.12
$[S_2Mo_{18}O_{62}]^{5-} + e^- \leftrightharpoons [S_2Mo_{18}O_{62}]^{6-}$	−0.11
$[S_2Mo_{18}O_{62}]^{6-} + e^- \leftrightharpoons [S_2Mo_{18}O_{62}]^{7-}$	−0.73
$[S_2Mo_{18}O_{62}]^{7-} + e^- \leftrightharpoons [S_2Mo_{18}O_{62}]^{8-}$	−0.91
$[LiS_2Mo_{18}O_{62}]^{5-} + e^- \leftrightharpoons [LiS_2Mo_{18}O_{62}]^{6-}$	−0.56
$[LiS_2Mo_{18}O_{62}]^{6-} + e^- \leftrightharpoons [LiS_2Mo_{18}O_{62}]^{7-}$	−0.67
$[Li_2S_2Mo_{18}O_{62}]^{5-} + e^- \leftrightharpoons [Li_2S_2Mo_{18}O_{62}]^{6-}$	−0.60
Chemical reactions [d]	K/M^{-1}
$[S_2Mo_{18}O_{62}]^{6-} + Li^+ \leftrightharpoons [LiS_2Mo_{18}O_{62}]^{5-}$	10^1 (K_1)
$[S_2Mo_{18}O_{62}]^{7-} + Li^+ \leftrightharpoons [LiS_2Mo_{18}O_{62}]^{6-}$	5×10^2 (K_2)
$[S_2Mo_{18}O_{62}]^{8-} + Li^+ \leftrightharpoons [LiS_2Mo_{18}O_{62}]^{7-}$	10^6 (K_3)
$[LiS_2Mo_{18}O_{62}]^{6-} + Li^+ \leftrightharpoons [Li_2S_2Mo_{18}O_{62}]^{5-}$	10^3 (K_4)
$[LiS_2Mo_{18}O_{62}]^{7-} + Li^+ \leftrightharpoons [Li_2S_2Mo_{18}O_{62}]^{6-}$	8×10^3 (K_5)

[a] See text and Fig. 9 for value of other input parameters.
[b] Diffusion coefficient used in the simulation was 1.4×10^{-5} cm^2 s^{-1} for Li^+ and 6.4×10^{-6} cm^2 s^{-1} for all polyoxo anions.
[c] Reversible charge transfer process simulated by use of value of 10^4 cm s^{-1} for the heterogeneous charge transfer rate constant (k_s) and 0.5 for the charge transfer (α).
[d] Reversible conditions achieved by making the rate constant for both forward (k_f) and reverse (k_b) reaction of homogeneous chemical reactions extremely fast.

4. The combination of E_5–E_7, K_3 and K_2 (Table 5) were chosen to give the best fit, while K_1, K_4–K_5 were automatically determined from other reactions, since these are the thermodynamically superfluous reactions discussed by Feldberg et al. [27].
5. The value of uncompensated resistance (R_u) of 250 Ω was used.
6. The double layer capacitance(C_{dl}) of 1×10^{-6} F cm^{-2} was used. Initially this value was allowed to vary until the theoretical and experimental results agreed satisfactorily.
7. Parameters $E_{1/2}$ and $K = k_f/k_b$ used in the simulation are listed in Table 6.
8. Ion pairng with the NBu_4^+ cation is neglected.

In Fig. 9(a), the simulation in the absence of Li^+ is attempted only for the first three reduction processes. Thus, the fourth process, which contains contributions from protonation of the four-electron reduced species in 95:5 $CH_3CN + H_2O$ (v/v) [25] and the minor process observed between processes **b** and **c** are not included in the simulation or in reaction Scheme 1. Excellent agreement between experiment and theory was obtained for the initial four electron transfer steps when Li^+ concentrations were examined in the range 0.2–0.5 mM and scan rates of between 0.10 and 1.0 V s^{-1} were used. This success of the simulation validated the assumptions that the heterogeneous and homogeneous rates involved in Scheme 1 were very fast relative to the voltammetric time scale and that all the redox processes are diffusion controlled under the conditions examined.

The success of the simulation in describing the voltammetry when Li^+ is present supports the hypothesis that the initial four one-electron reversible charge transfer processes detected when 0.1 M NBu_4ClO_4 is the electrolyte, still occur when Li^+ is added. However, in the presence of $LiClO_4$, the two-electron reduced product $[S_2Mo_{18}O_{62}]^{6-}$ interacts with Li^+ to generate $[LiS_2Mo_{18}O_{62}]^{5-}$ (Eq. (8), Table 6):

$$[S_2Mo_{18}O_{62}]^{6-} + Li^+ \leftrightharpoons [LiS_2Mo_{18}O_{62}]^{5-} \quad (K_1 = 10^1\ M^{-1}) \tag{8}$$

In contrast, the even more basic, three-electron reduced species $[S_2Mo_{18}O_{62}]^{7-}$ is involved in an equilibrium favoring $[Li_2S_2Mo_{18}O_{62}]^{5-}$ over $[LiS_2Mo_{18}O_{62}]^{6-}$:

$$[S_2Mo_{18}O_{62}]^{7-} + Li^+ \leftrightharpoons [LiS_2Mo_{18}O_{62}]^{6-} \quad (K_2 = 5\times10^2\ M^{-1}) \tag{9}$$

$$[LiS_2Mo_{18}O_{62}]^{6-} + Li^+ \leftrightharpoons [Li_2S_2Mo_{18}O_{62}]^{5-} \quad (K_4 = 7\times10^3\ M^{-1}) \tag{10}$$

Finally, the extremely basic four-electron reduced species $[S_2Mo_{18}O_{62}]^{8-}$ even more strongly favors the doubly lithiated ion $[Li_2S_2Mo_{18}O_{62}]^{6-}$ over the singly lithiated $[LiS_2Mo_{18}O_{62}]^{7-}$:

$$[S_2Mo_{18}O_{62}]^{8-} + Li^+ \leftrightharpoons [LiS_2Mo_{18}O_{62}]^{7-} \quad (K_3 = 10^6\ M^{-1}) \tag{11}$$

$$[LiS_2Mo_{18}O_{62}]^{7-} + Li^+ \leftrightharpoons [Li_2S_2Mo_{18}O_{62}]^{6-} \quad (K_5 = 8\times10^3\ M^{-1}) \tag{12}$$

Phenomenologically, the reactions between reduced forms of $[S_2Mo_{18}O_{62}]^{4-}$ and Li^+ are analogous to those with H^+, with the acidity strength being in the order of $HClO_4 > LiClO_4 > H_2O$. Thus, in the presence of 5% H_2O, the primary processes **III** and **IV** are shifted towards a more positive potential and became closer to each other, but do not merge. In the presence of 0.1 M $LiClO_4$, processes **III** and **IV** merge and are observed as an overall chemically reversible two-electron process, whilst processes **I** and **II** remain separated in the presence of H_2O or $LiClO_4$. In contrast, processes **I**, **II**, **III** and **IV** eventually merge to give two chemically reversible two-electron process in the presence of $HClO_4$. Consequently, the role of Li^+, frequently contained in the electrolyte [19,20,28], cannot be assumed to be thermodynamically innocent in studies of polyoxometalates, nor can the solvent (CH_3CN or H_2O) [29–31], nor even presumably $[NBu_4]^+$, as ion-pairs are always likely to be significant when highly negative species are generated at electrode surfaces. Finally, it needs to be noted that as with all simulations of data involving a significant number of unknown parameters, it cannot be assumed that a unique data set has been obtained. For all these reasons, the physical significance of the exact values of equilibrium constants K_1–K_5 in Eqs. (8)–(12) are unclear, although clearly a simple model

based solely on electrostatic interactions will not provide an adequate explanation of this data set.

References

[1] C.L. Hill, C.M. Prosser-McCartha, Coord. Chem. Rev. 143 (1995) 407.
[2] J.T. Rhule, C.L. Hill, D.A. Judd, Chem. Rev. 98 (1998) 327.
[3] N. Mizuno, M. Misono, Chem. Rev. 98 (1998) 199.
[4] A.R. Seidle, R.A. Newmark, R.P. Brown-Wensley, R.P. Skarjune, L.C. Haddad, K.O. Hodgson, A.L. Roe, Organometallics 7 (1988) 2078.
[5] A.R. Seidle, R.A. Newmark, W.B. Gleason, R.P. Skarjune, K.O. Hodgson, A.L. Roe, V.B. Day, Solid State Ionics 26 (1988) 109.
[6] T. Yamase, H. Fujita, K. Fukushima, Inorg. Chim. Acta 151 (1988) 15.
[7] D. Attanasio, L. Suber, Inorg. Chem. 28 (1989) 3779.
[8] L.A. Combs-Walker, C.L. Hill, J. Am. Chem. Soc. 114 (1992) 938.
[9] C.L. Hill, Synlett (1995) 127.
[10] B.S. Jaynes, C.L. Hill, J. Am. Chem. Soc. 115 (1993) 12212.
[11] R.F. Renneke, C.L. Hill, J. Am. Chem. Soc. 110 (1988) 5461.
[12] R.F. Renneke, M. Kadkhodayan, M. Pasquali, C.L. Hill, J. Am. Chem. Soc. 113 (1991) 8357.
[13] R.F. Renneke, M. Pasquali, C.L. Hill, J. Am. Chem. Soc. 112 (1990) 6585.
[14] D. Satire, C.L. Hill, J. Chem. Soc. Chem. Commun. (1990) 634.
[15] M.T. Pope, Heteropoly and Isopoly Oxometalates, Springer, New York, 1983.
[16] B. Cartié, J. Chem. Res. S (1988) 290.
[17] E. Papaconstantinou, M.T. Pope, Inorg. Chem. 6 (1967) 1152.
[18] G.A. Tsigdinos, C.J. Hallada, J. Less Common Met. 9 (1970) 667.
[19] B. Keita, L. Nadjo, J. Electroanal. Chem. 227 (1987) 77.
[20] B. Keita, L. Nadjo, J. Electroanal. Chem. 217 (1987) 287.
[21] S. Himeno, K. Maeda, T. Osakai, A. Saito, T. Hori, Bull. Chem. Soc. Jpn. 66 (1993) 109.
[22] S. Himeno, T. Osakai, A. Saito, J. Electroanal. Chem. 337 (1992) 371.
[23] J.B. Cooper, D.M. Way, A.M. Bond, A.G. Wedd, Inorg. Chem. 32 (1993) 2416.
[24] D.M. Way, A.M. Bond, A.G. Wedd, Inorg. Chem. 36 (1997) 2826.
[25] D.M. Way, J.B. Cooper, M. Sadek, T. Vu, P.J. Mahon, A.M. Bond, R.C. Brownlee, A.G. Wedd, Inorg. Chem. 36 (1997) 4227.
[26] P.D. Prenzler, C. Boskovic, A.M. Bond, A.G. Wedd, Anal. Chem. 71 (1999) 3650.
[27] M. Rudolph, D.P. Reddy, S.W. Feldberg, Anal. Chem. 66 (1994) 589A.
[28] B. Keita, L. Nadjo, J. Electroanal. Chem. 230 (1987) 267.
[29] R.A. Robinson, R.H. Stokes, Electrolyte Solutions, Butterworths Scientific, London, 1959.
[30] R.R. Dogonadze, E. Kálmán, A.A. Kornyshev, J. Ulstrup, The Chemical Physics of Solvation, Part A: Theory of Solvation, Elsevier, New York, 1985.
[31] B. Keita, D. Bouazi, L. Nadjo, J. Electrochem. Soc. 135 (1988) 87.